Molecular Membrane Biology, May–June 2006; 23(3): 277–288

Taylor & Francis
Taylor & Francis Group

Curvature-dependent lateral distribution of raft markers in the human erythrocyte membrane

HENRY HÄGERSTRAND[1], LUCYNA MRÓWCZYŃSKA[2], ULRICH SALZER[3], RAINER PROHASKA[3], KIMMO A. MICHELSEN[1], VERONIKA KRALJ-IGLIČ[4,5], & ALEŠ IGLIČ[4]

[1]*Department of Biology, Åbo Akademi University, Åbo/Turku, Finland,* [2]*Department of Cell Biology, A.Mickiewicz University, Poznan, Poland,* [3]*Department of Medical Biochemistry, Medical University of Vienna, Max F. Perutz Laboratories, Vienna, Austria,* [4]*Laboratory of Physics, Faculty of Electrical Engineering, University of Ljubljana, Ljubljana, Slovenia, and* [5]*Institute of Biophysics, Faculty of Medicine, University of Ljubljana, Ljubljana, Slovenia*

(Received 10 November 2005; and in revised form 23 February 2006)

Abstract
The distribution of raft markers in curved membrane exvaginations and invaginations, induced in human erythrocytes by amphiphile-treatment or increased cytosolic calcium level, was studied by fluorescence microscopy. Cholera toxin subunit B and antibodies were used to detect raft components. Ganglioside GM1 was enriched in membrane exvaginations (spiculae) induced by cytosolic calcium and amphiphiles. Stomatin and the cytosolic proteins synexin and sorcin were enriched in spiculae when induced by cytosolic calcium, but not in spiculae induced by amphiphiles. No enrichment of flotillin-1 was detected in spiculae. Analyses of the relative protein content of released exovesicles were in line with the microscopic observations. In invaginations induced by amphiphiles, the enrichment of ganglioside GM1, but not of the integral membrane proteins flotillin-1 and stomatin, was observed. Based on the experimental results and theoretical considerations we suggest that membrane skeleton-detached, laterally mobile rafts may sort into curved or flat membrane regions dependent on their intrinsic molecular shape and/or direct interactions between the raft elements.

Keywords: *Erythrocyte, membrane microdomain, raft, membrane curvature, intrinsic curvature, amphiphile, calcium ionophore A23187*

Introduction

The normal discoid shape of human erythrocytes (discocyte) can be transformed under the influence of different agents to a crenated shape (echinocyte), characterized by membrane protrusions or spiculae emerging from a rounded cell body, or an invaginated shape (stomatocyte). These shape transformations can further lead to the formation of exovesicles and endovesicles, respectively. The bilayer-couple hypothesis by Sheetz and Singer proposed that these shape changes were due to small surface area changes of one of the membrane leaflets (Sheetz & Singer 1976). A strong theoretical support for this hypothesis has been provided (Iglič 1997, Iglič & Hägerstrand 1999, Mukhopadhyay et al. 2002, Lim et al. 2002). In line with the bilayer-couple hypothesis is the finding that cationic amphiphiles, which preferentially partition in the inner leaflet due to the higher amount of negatively charged lipids, induce a stomatocytic shape whereas anionic amphiphiles induce an echinocytic shape (Deuticke 1968, Hägerstrand et al. 2004). Echinocytic shape transformation and the release of exovesicles can also be induced by intrinsic membrane processes associated with the rise of cytosolic calcium (Allan et al. 1980). This calcium-induced shape change is probably due to a calcium dependent scramblase activity mediating the redistribution of membrane phospholipids between the inner and the outer membrane leaflets (Lin et al. 1994). The translocation rate for sphingomyelin, a membrane lipid preferentially located at the outer leaflet, is much slower than for glycerophospholipids which is thought to be the cause of the expansion of the outer membrane leaflet and the echinocytic shape transformation (Smeets et al. 1994, Kamp et al. 2001). However, other calcium-induced processes such as the breakdown of phosphoinositides and cell volume shrinking might also

Correspondence: Henry Hägerstrand, Department of Biology, Åbo Akademi University, Biocity, FIN-20520, Åbo/Turku, Finland. Fax: +358-2-2154748. E-mail: henry.hagerstrand@abo.fi

ISSN 0968-7688 print/ISSN 1464-5203 online
DOI: 10.1080/09687860600682536

contribute to the shape change (Allan & Thomas 1981).

Rafts have been described as mobile sphingolipid- and cholesterol-based microdomains in the membrane that vary in composition and size (6–50 nm in diameter) (Pralle et al. 2000, Prior et al. 2003, Sharma et al. 2004, Plowman et al. 2005). They host specific proteins and can coalesce into larger, functional domains (Simons & Toomre 2000, Simons & Vaz 2004). The existence of independent inner membrane leaflet rafts with different physical properties than those in the outer leaflet has also been indicated (Devaux & Morris 2004). Rafts are thought to play roles in budding and vesicle formation associated with endocytic and exocytic transport routes (Ikonen 2001, Huttner & Zimmerberg 2001). The local clustering of rafts, with a preference for high spherical curvature, and the concomitant local shape changes may be strongly coupled as a part of the driving mechanism of the vesicle budding. In human erythrocytes, recruitment of raft-associated components has been reported in membrane exovesicles induced by increased intracellular calcium level (C-vesicles) (Salzer et al. 2002) and in malarial endovacuoles (Murphy et al. 2004). While malarial vacuolar invaginations are enriched in the integral raft protein flotillin-1 (Murphy et al. 2004), enrichment of integral raft protein stomatin and cytosolic proteins sorcin and synexin was detected in C-vesicles (Salzer et al. 2002). These findings are in line with the concept of coexistence of compositionally distinct lipid microdomains in a given membrane (Ikonen 2001) and may be taken to indicate a sorting of raft components due to inward or outward membrane curvature.

To shed further light on the preference of different rafts for inward or outward membrane curvature, we studied by fluorescence microscopy the distribution of raft markers in human erythrocyte membrane exvaginations and invaginations induced by amphiphilic compounds or increased cytosolic calcium level. In addition, the relative abundance of some raft and non-raft associated membrane proteins in released erythrocyte exovesicles was studied.

Materials and methods

Chemicals

Chlorpromazine hydrochloride (C-8138), Triton X-100 (T-8787), ionophore A23187 (C-7522), and fish skin gelatin (Fsg, G-7041) were obtained from Sigma, 3-(dodecyldimethylammonio)-1-propanesulphonate (dodecylzwittergent^{R}, 693015) from Calbiochem and dodecylmaltoside (44205) from Fluka. Cholera toxin subunit B-Alexa (CT-B, C-34776), Bodipy FL C_5-ganglioside GM1 (GM1-BODIPY, B-13950) and Alexa-rabbit anti-mouse IgG (A-11029) were from Molecular Probes. Monoclonal antibody against stomatin is described in Hiebl-Dirschmied et al. (1991). Monoclonal antibodies against flotillin-1 (610820) and synexin (annexin VII, 610668) were from BD Biosciences Pharmingen, monoclonal antibody against sorcin (33-8000) from Zymed and monoclonal antibodies against band 3 (B-9277) and spectrin (S-3396) from Sigma.

Isolation of erythrocytes

Blood was drawn from the authors (H.H., L.M.) and other healthy donors by venipuncture into heparinized tubes. Blood was washed three times with buffer (145 mM NaCl, 5 mM KCl, 4 mM Na_2HPO_4, 1 mM NaH_2PO_4, 1 mM $MgSO_4$, 1 mM $CaCl_2$, 10 mM glucose, pH 7.4). Erythrocytes were suspended in the buffer at a cell density of 1.65×10^9 cells/ml. Cells were stored at $+4^{\circ}$C and used usually within 5 h.

Staining with raft markers

For CT-B (and GM1-BODIPY) staining in invaginated erythrocytes, cells (1.65×10^8 cells/ml, $\sim$1.5% haematocrit) were blocked with Fsg (1%, 30 min, room temperature (RT)), stained with CT-B (1 μg/μl in the buffer, 1/125, 15 min, RT) or GM1-BODIPY (0.5 μg/μl in dimethylsulfoxide, 1/100, 30 min, RT), washed twice and treated with amphiphile. 7 μl of the cell suspension was settled (10 min, RT) on a polylysine-treated (0.1 mg/ml, 10 min, washing and drying) cover glass and fixed in 3% paraformaldehyde (PFA) on ice for 20 min. After washing, cells were mounted on 80% glycerol. The cover slips were sealed with nail polish.

For CT-B and GM1-BODIPY staining in exvaginated cells, erythrocytes were treated with amphiphile or A23187 and fixed in 3% PFA on ice for 30 min. Following staining with CT-B or GM1-BODIPY as above, cells were washed twice, settled, washed and mounted.

For flotillin-1, stomatin, sorcin and synexin staining, cells were treated with amphiphile or A23187. Cells were fixed in 3% PFA on ice for 5 min and then fixed and permeabilized in dry methanol on ice for 10 min. Following washing, cells were settled on polylysine-treated cover glasses and washed. After blocking and washing as above, cells were incubated with the primary antibody (1/20 for flotillin-1, stomatin, synexin, 1/100 for sorcin, 60 min, RT). After washing, cells were incubated with the fluorophore conjugated secondary antibody (1/200,

0.05% Fsg, 60 min, RT). After washing, cover slips were mounted as above.

Amphiphile and A23187 treatment

Erythrocytes were treated with stomatocytogenic amphiphiles ($\leq$130 μM chlorpromazine or $\leq$0.008% Triton X-100, 60 min, 37°C) or echinocytogenic amphiphiles ($\leq$263 μM dodecylzwittergent or $\leq$44 μM dodecylmaltoside, 30 min, 37°C) or ionophore A23187 ($\leq$10 μM, 5–10 min, 37°C, calcium 1-3.8 mM) at sublytic concentrations previously shown to induce either membrane invagination (stomatocytosis) and formation of endovesicle-like invaginations, or membrane exvagination (echinocytosis, spiculation) and formation of exovesicles (Hägerstrand & Isomaa 1989, 1992, Hägerstrand et al. 2000), respectively. The morphology of treated erythrocytes was checked by transmission light microscopy.

Microscopy

Samples from several separate experiments were studied using a Leica DM RXA microscope (100 ×/1.4 aperture immersion oil objective, 10 × ocular). Treated stained cells were compared to untreated stained cells and cells treated with the secondary antibody only. Images were acquired with a Leica DC300F CCD-camera. Transmission and scanning electron microscopy was performed as previously described (Hägerstrand & Isomaa 1992).

Preparation of exovesicles

C-vesicles (also termed microvesicles) were prepared as described (Salzer et al. 2002) with slight modifications. Briefly, erythrocytes were resuspended in 9 volumes TBS (10 mM Tris-Cl, 150 mM NaCl, pH 7.5) containing 100 μM $CaCl_2$ and 5μM ionophore A23187 and incubated at 37°C for 30 min with constant shaking. After addition of EDTA to a final concentration of 5 mM, the erythrocytes were pelleted at 15,000 *g* for 25 sec. The supernatant was centrifuged at 15,000 *g* for 30 min and the pelleted C-vesicles were washed once in TBS and then resuspended in an appropriate volume of TBS for further analysis.

Dodecylmaltoside-induced vesicles (M-vesicles) and dodecylzwittergent-induced vesicles (Z-vesicles) were prepared as described (Hägerstrand & Isomaa 1989) with slight modifications. Briefly, erythrocytes were resuspended in TBS containing either 40 μM dodecylmaltoside or 268 μM dodecylzwittergent at a haematocrit of 1.5% and incubated at 37°C with constant shaking for 30 min. Erythrocytes were pelleted at 2,500 g for 10 min and the resulting supernatant was centrifuged at 27,000 *g* for 40 min. The pelleted M- or Z-vesicles were washed once in TBS and then resuspended in an appropriate volume of TBS for further analysis.

Protein analyses

Protein samples were analyzed by gel electrophoresis, silver staining, immunoblotting with the indicated antibodies, and determination of acetylcholinesterase (AChE) activity, respectively, as previously described (Salzer et al. 2002).

Results

Shape alteration

Certain amphiphilic compounds like dodecylmaltoside and dodecylzwittergent, as well as an increased cytosolic calcium level, induce membrane exvagination (echinocytosis, spiculation), including budding and release of small exovesicles in human erythrocytes, while other amphiphilic compounds like chlorpromazine and Triton X-100 induce large membrane invaginations (stomatocytosis) and formation of small endovesicle-like invaginations. Figure 1A shows the exvaginated shape of erythrocytes treated with ionophore A23187 plus calcium. The spiculae are distributed around the spheroid main body of the cell. Membrane buds, apparently in the process of being released, can be seen on the tips of spiculae. Figure 2A shows that virtually all cells in a chlorpromazine-treated population contain small endovesicle-like invaginations. These are often concentrated in the large primary stomatocytic pocket (invagination).

Raft markers and exvagination

A marked enrichment of stomatin, sorcin, and synexin was detected in calcium-induced erythrocyte spiculae (Figure 1B1, 1C1 and 1D1). Particularly sorcin and synexin appear to accumulate on the tips of spiculae. In spiculae induced by dodecylmaltoside and dodecylzwittergent no increased level of stomatin, sorcin or synexin was observed (Figure 1B2, 1B3, 1C3 and 1D2). A patchy appearance of stomatin on the spheroid main body of amphiphile-treated erythrocytes indicates that membrane aggregation of stomatin had occurred (Figure 1B2, dodecylmaltoside). Signs of membrane patching (and binding) of sorcin and synexin were observed in amphiphile-treated cells at high amphiphile concentrations (Figure 1C3 inset, sorcin/dodecylmaltoside). This is apparently due to calcium leakage into the cells. There was no consistent enrichment of flotillin-1 detected in calcium- or amphiphile-

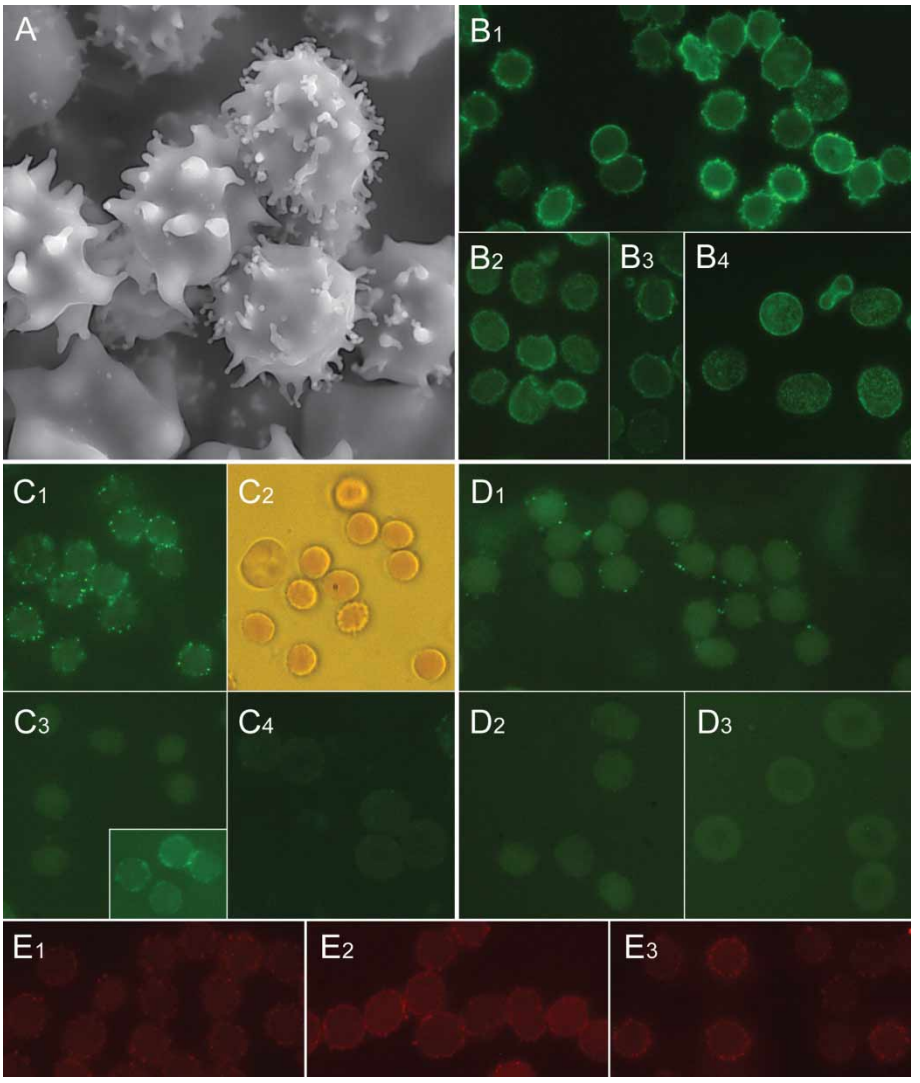

Figure 1. Distribution of raft markers in human erythrocyte membrane exvaginations (spiculae).
Scanning electron micrograph showing exvaginated human erythrocytes following incubation with ionophore A23187 (1 μM, 10 min, 37°C) in the presence of 3.8 mM calcium (A). Immunocytochemical detection of stomatin in erythrocytes treated with A23187 plus calcium (B1), dodecylmaltoside (B2), dodecylzwittergent (B3) and untreated (B4). Immunocytochemical detection of sorcin in erythrocytes treated with A23187 plus calcium (C1), dodecylmaltoside (C3, in inset permeable cells) and untreated (C4). C2 is a transmission light micrograph showing the mainly sphero-echinocytic shape of erythrocytes shown in C1. Immunocytochemical detection of synexin in erythrocytes treated with A23187 plus calcium (D1), dodecylmaltoside (D2) and untreated (D3). Detection of ganglioside GM1 by cholera toxin subunit B staining of erythrocytes treated with ionophore A23187 plus calcium (E1), dodecylzwittergent (E2) and dodecylmaltoside (E3). Notably, the magnification is larger in A than in other micrographs. This Figure is reproduced in colour in *Molecular Membrane Biology* online.

induced spiculae, however, these treatments induced membrane patching of flotillin-1 on the spheroid main body of the cell (not shown, Figure 2D1). In both, calcium- and amphiphile-treated cells, as well as ATP-depleted cells (not shown), enrichment of CT-B in spiculae was indicated (Figure 1E1, 1E2 and 1E3). This enrichment appeared most obvious in calcium-treated cells. GM1-BODIPY stained spiculae of calcium- and amphiphile-treated cells, but no enrichment was detected (not shown). Thus, GM1-BODIPY is not a marker of rafts sorting into outward curved membranes. It should be noted that in all of the studied spiculated cells some exovesiculation has probably already occurred.

Raft markers and invagination

Our experiments indicate that the ganglioside GM1-staining raft marker CT-B (Harder et al. 1998) and GM1-BODIPY (Janes et al. 1999) distribute and even enrich in invaginations induced by chlorpromazine (Figure 2B1 and 2C1) and Triton X-100 (Figure 2C2). No enrichment of flotillin-1 (Figure 2D1) or stomatin (Figure 2E1), sorcin or synexin

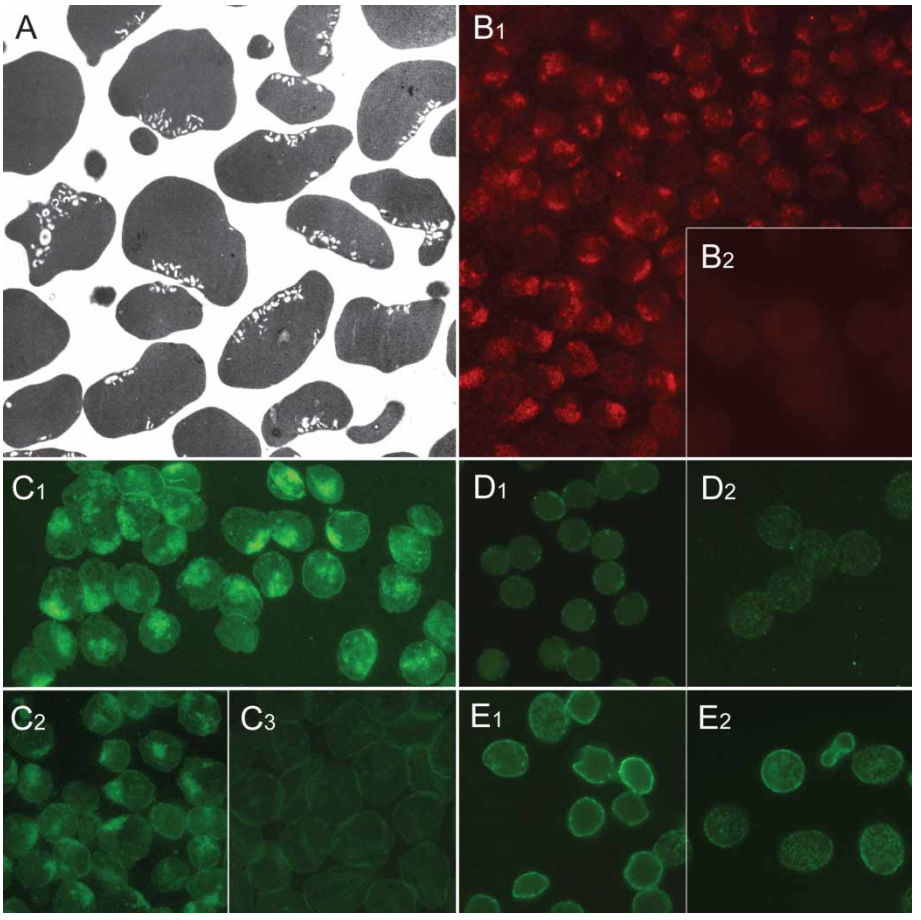

Figure 2. Distribution of raft markers in human erythrocyte membrane invaginations. Transmission electron micrograph showing invaginated human erythrocytes following incubation with chlorpromazine (100 μM, 60 min, 37°C) (A). Clustered endovesicle-like invaginations are seen. Cholera toxin subunit B staining of gangliosides in erythrocytes treated with chlorpromazine (B1) and untreated cells (B2). Ganglioside GM1-BODIPY staining of erythrocytes treated with chlorpromazine (C1), Triton X-100 (C2) and untreated cells (C3). Immunocytochemical detection of flotillin-1 in erythrocytes treated with chlorpromazine (D1) and untreated cells (D2). Immunocytochemical detection of stomatin in erythrocytes treated with chlorpromazine (E1) and untreated cells (E2). Notably, the magnification is larger in A than in other micrographs. This Figure is reproduced in colour in *Molecular Membrane Biology* online.

(not shown), was detected in chlorpromazine-induced invaginations. A patchy appearance of flotillin-1 and stomatin in chlorpromazine-treated cells indicates the membrane coalescence of flotillin-1 and stomatin (Figure 2D1 and 2E1). In some instances, flotillin-1 seemed to sort around the mouth of the primary stomatocytic invaginated pocket (not shown). In control cells, CT-B and GM1-BODIPY had an even, highly dispersed distribution (Figure 2B2 and 2C3), while flotillin-1 and stomatin showed a dotted distribution (Figure 2D2 and 2E2).

Raft markers and exovesiculation

In order to study the differential segregation of membrane proteins during dodecylmaltoside-, dodecylzwittergent- and calcium-treatment by a complementary method, we isolated exovesicles shed by the erythrocytes upon these treatments and compared the relative amounts of several membrane marker proteins (Figure 3). As most of the exovesicles probably originate from the tips of membrane protrusions (Kralj-Iglič et al. 2005), the membrane protein content of the released vesicle reflects the local membrane protein composition of the protrusions' tips. The protein composition of the different vesicles and the parent erythrocyte membranes is shown in Figure 3. In accordance with previous results (Allan et al. 1980, Hägerstrand & Isomaa 1994, Salzer et al. 2002), the glycosylphosphatidylinositol (GPI)-anchored protein AChE, which is a raft marker located at the exoplasmic side of the membrane, is found to be highly enriched in all three types of highly curved exovesicles. The vesicular aliquots were normalised to AChE activity to show the differences in the depletion of the respective proteins relative to this raft marker. All types of

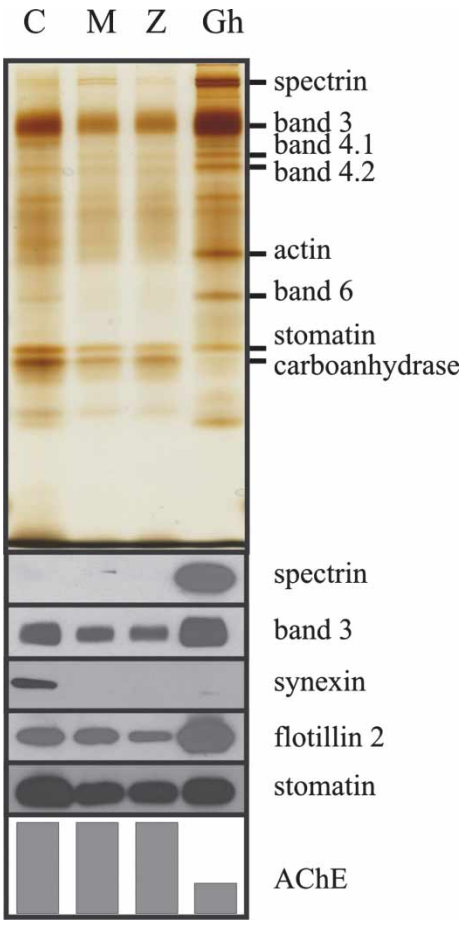

Figure 3. Different membrane protein composition of ghosts compared to M-, Z- and C-vesicles.
Erythrocytes were treated with dodecylmaltoside, dodecylzwittergent, or calcium/A23187, and the vesicles were prepared as described in the text. C-vesicles (C), M-vesicles (M), Z-vesicles (Z) and erythrocyte membranes (Gh) were analysed for AChE activity. Aliquots of the vesicles (normalized to AChE activity) and of the erythrocyte membranes (containing one third of the vesicular AChE activity (lowest panel in arbitrary units)) were analysed by 11% polyacrylamide gel electrophoresis/silver staining (upper panel), and immunoblotting (lower panels), as indicated. This Figure is reproduced in colour in *Molecular Membrane Biology* online.

vesicles are strongly depleted of the peripheral membrane protein band 6 and the membrane skeletal components spectrin, band 4.1, band 4.2 and actin (Figure 3, silverstain). Band 3 and the major integral raft components stomatin and flotillin-2 are present in the vesicles (Figure 3, Western blot), however, the different relative amounts of these proteins in the vesicles indicate a differential segregation of these components during the vesiculation processes. The relative abundance of these proteins in vesicles and ghosts was assessed by quantitative Western blotting (data not shown) and the respective protein/AChE ratios were calculated (Table I). Flotillin-2 is similarly depleted in all three types of vesicles and band 3 is more abundant in C- than in M- and Z-vesicles. The stomatin/AChE ratio in C-vesicles is three times higher than in M- and Z-vesicles. This different vesicular abundance of stomatin corroborates the microscopy data, showing that stomatin is enriched in the calcium-induced spiculae but not in spiculae obtained after dodecylmaltoside or dodecylzwittergent treatment. Synexin is present in C-vesicles but absent from untreated erythrocyte membranes and M- and Z-vesicles, thereby indicating that an elevated cytosolic calcium level is a prerequisite to its membrane and vesicular localization.

Discussion

To learn about the principles governing the lateral segregation and the organization of erythrocyte rafts, we investigated the distribution of raft markers in erythrocyte membrane exvaginations induced by different echinocytogenic stimuli, and also their relative enrichment in the released exovesicles. Our results show that these stimuli, that is amphiphile-treatment or increased cytosolic calcium level, affect the sorting of raft components during exvagination (Table II) and subsequent vesicle release (Table I) in a different manner.

In this work we suggest that membrane curvature is a driving mechanism for the lateral segregation of different rafts. As outlined in the Appendix, laterally mobile membrane components preferentially distribute into energetically favorable curved membrane regions according to the intrinsic shape of the molecule or the molecular ensemble (Figure 4). Additionally, attractive forces between the rafts may further enhance the segregation process leading to the formation of larger raft domains within the

Table I. Differential segregation of membrane proteins into erythrocyte vesicles.

	Ghosts	Z-vesicles	M-vesicles	C-vesicles
Band 3/AChE	1.00	0.07 ± 0.02	0.10 ± 0.02	0.15 ± 0.04
Flotillin-2/AChE	1.00	0.07 ± 0.03	0.10 ± 0.02	0.10 ± 0.04
Stomatin/AChE	1.00	0.20 ± 0.05	0.20 ± 0.05	0.60 ± 0.10

Quantitative immunoblotting was performed to assess the relative amounts of the respective proteins in the vesicles and ghosts. The relative protein/AChE ratios in the vesicles were calculated in relation to the respective ratios in ghosts which are arbitrarily set to 1.00. Values were generated from 3 independent experiments; standard deviations are shown by ±.

Table II. Accumulation of raft markers in human erythrocyte exvaginations and invaginations as studied by fluorescence microscopy.

	Exvaginations (spiculae)		Invaginations
	Amphiphile (dodecylzwittergent and dodecylmaltoside)	Intracellular Calcium (A23187)	Amphiphile (chlorpromazine)
CT-B	+	+	+
GM1-BODIPY	−	−	+
Flotillin-1	−	−	−
Stomatin	−	+	−
Sorcin	−	+	−
Synexin	−	+	−

Indications on (+) enrichment or (−) no enrichment (but in some cases presence) of raft markers in human erythrocyte exvaginations and invaginations induced by amphiphiles or A23187 plus calcium.

curved membrane region (Appendix). However, apart from membrane curvature, cytoskeletal attachment has also to be considered as a factor influencing the depletion of membrane components from the membrane skeleton-free membrane protrusions (Liu et al. 1989) and exovesicles (Allan et al. 1976, Hägerstrand & Isomaa 1994). For example, the relative depletion of the band 3 protein from C-vesicles can be directly correlated with the amount of membrane skeleton-associated, and therefore laterally immobile, band 3 protein (Hagelberg & Allan 1990).

The raft markers under investigation can be grouped into three classes according to their membrane anchorage and topology. The lipid or lipid-bound raft markers GM1 and AChE, that are located at the exoplasmic membrane leaflet, stomatin and the flotillins, that are the major integral protein raft-components and are exclusively exposed at the cytoplasmic side of the membrane, and synexin and sorcin, that have been shown to translocate from the cytosol to the membrane upon calcium-binding and are major components of vesicular rafts (Salzer et al. 2002).

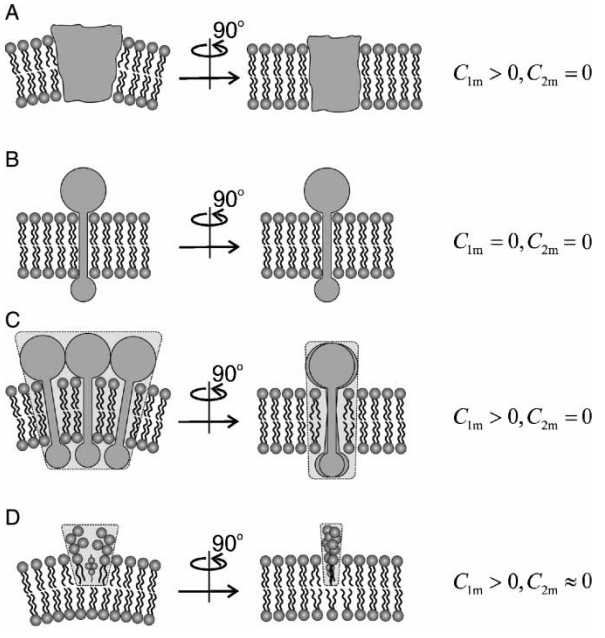

Figure 4. Intrinsic shapes of membrane components. Schematic figure of different intrinsic shapes (characterized by two intrinsic curvatures C_{1m} and C_{2m}) of membrane components which may be single molecules (A,B) or small complexes of molecules (C,D). Shapes A, C and D are anisotropic, shape B is isotropic.

The GPI-anchored protein AChE has been shown to accumulate both in C-vesicles (Allan et al. 1980) and amphiphile-induced vesicles (Hägerstrand & Isomaa 1994 and references therein) and to be present in rafts of C-vesicles together with stomatin, synexin, sorcin and GM1 (Salzer et al. 2002). The highly specific enrichment of AChE in amphiphile and calcium-induced exovesicles can be seen in Figure 3 and Table I. The microscopic studies indicate that also ganglioside GM1 enriches in calcium- and amphiphile-induced spiculae (Figure 1E1, 1E2 and 1E3). Together, these data suggest that GM1- and AChE-rich rafts accumulate in membrane spiculae irrespective of the echinocytogenic stimulus, thereby indicating a high mobility of these types of rafts at the exoplasmic membrane leaflet. The enrichment of GM1 at the tips of the echinocyte spiculae and in highly curved exovesicles is energetically favourable due to the intrinsic conical shape of GM1 (Hirai et al. 1998, 2003), characterized by positive intrinsic curvatures $C_{1m} > 0$ and $C_{2m} > 0$ (see Figure 4 for definition of C_{1m} and C_{2m}). Similarly, an intrinsic conical shape can also be assumed for AChE, where a bulky 75 kDa protein mass is anchored to the outer membrane bilayer by a single phospholipid (GPI). It can therefore be expected that the coalescence of GM1- and AChE-containing rafts in the outer leaflet of membrane exvaginations (spiculae, buds) and of exovesicles is promoted by their intrinsic conical shapes and probably, additionally, by direct interaction (see also Appendix).

We show that stomatin is markedly enriched in spiculae of A23187/calcium treated erythrocytes (Figure 1B1) and C-vesicles (Figure 3, Table I), in

accordance with previous results (Salzer et al. 2002, Salzer & Prohaska 2003). However, no enrichment of stomatin in spiculae and vesicles is found when cells are treated with echinocytogenic amphiphiles (Figure 1B2 and 1B3, Figure 3, Table I). These findings suggest that also other factors than outward membrane curvature affect the enrichment of stomatin in membrane protrusions. Several speculative possibilities can be envisaged. (i) Stomatin-specific rafts are anchored to the membrane skeleton. The co-isolation of raft markers and cytoskeletal components in detergent-resistant membranes suggests an interaction between the membrane skeleton and lipid rafts (U.S. and R.P., unpublished observations). Upon A23187/calcium treatment the stomatin-rafts might detach from the membrane skeleton and become enriched in the spiculae. (ii) Alternatively, calcium-loading may induce specific modifications in stomatin-containing rafts which alter their intrinsic shape and render their accumulation in highly curved membrane regions energetically more favourable. Such a regulated intrinsic shape change of stomatin-specific rafts may be envisaged upon platelet activation. In resting platelets, stomatin is predominantly found on the cytosolic side of endovesicles, whereas on activation stomatin becomes enriched at the luminal side of exovesicles (Mairhofer et al. 2002).

Flotillins are absent from spiculae and vesicles irrespective of the echinocytogenic stimulus (Figure 3, Table I). This may again be due to an incompatible intrinsic membrane curvature of flotillin-specific rafts and/or cytoskeletal association; apart from the co-isolation of flotillins and membrane skeleton in detergent resistant membranes in erythrocytes, a link of flotillin-2 to the cortical actin cytoskeleton has also been suggested in other cells (Neumann-Giesen et al. 2004). Moreover, the patching of stomatin and flotillin-1 observed on the spheroid main body of amphiphile-treated cells suggests that amphiphiles may induce a coalescence of rafts into large aggregates which restrict their sorting into highly curved membrane regions (Figure 2D1, 2E1 and 1B2) (see also Harder et al. 1998 and Figure 5). In this process a direct interaction between rafts may play an important role (Appendix).

The calcium-dependent raft markers synexin and sorcin (Salzer et al. 2002) are found at the tips of the echinocyte spiculae in calcium/A23187-treated cells (Figure 1C1 and 1D1) and are present in C-vesicles (Figure 3) whereas upon amphiphile treatment, they are absent from both the membrane and vesicles (Figure 1C3, 1D2 and 3). Therefore, it can be concluded that synexin and sorcin may have a modulating but not crucial role in membrane budding and vesicle release. Concerning synexin, a similar conclusion was drawn from experiments with synexin-lacking mouse erythrocytes (Herr et al. 2003). Apart from C-vesicles (microvesicles, 180 nm in diameter), calcium-loaded erythrocytes shed a small amount of nanovesicles (80 nm in diameter). Synexin and sorcin were shown to be the major membrane and raft constituents of these nanovesicles (Salzer et al. 2002). What is the driving force behind this strong enrichment of synexin and sorcin-specific rafts in C-vesicles and especially in nanovesicles? In line with our theoretical considerations (see Appendix), the specific intrinsic curvatures of synexin might be a possible explanation. Structural analyses revealed that synexin (Liemann et al. 1997) – similar to other members of the annexin protein family (Rety et al. 2005) – has a slightly curved shape with the calcium- and membrane-binding site(s) lying on the convex side of the molecule. Synexin-specific rafts might thus have positive intrinsic curvatures (i.e., $C_{1m} > 0$ and/or $C_{2m} > 0$) (see also Figure 4) which may promote the accumulation of synexin-specific rafts at highly curved membrane regions of budding nanovesicles (Figure 5).

We also compared the distribution of raft markers in exvaginated erythrocytes to that in the invaginated cells (Table II). Membrane invaginations were induced in erythrocytes by stomatocytogenic amphiphiles (Hägerstrand et al. 2004) which are thought to induce membrane invaginations due to their preferential intercalation in the inner leaflet of the erythrocyte membrane and its consequent expansion with respect to the outer membrane leaflet (Sheetz &

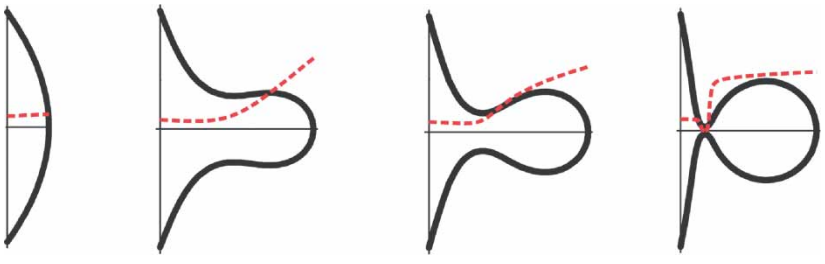

Figure 5. Accumulation of membrane components in the budding region. Relative concentration of membrane components (raft elements) characterized by positive $C_{1m} = C_{2m}$ and negative w during the budding/vesiculation of the membrane is shown (dotted line). See the Appendix for details.

Singer 1976). Our results indicated that the raft component GM1 distributes and even enriches in these invaginations (Figure 2B1, 2C1 and 2C2). Since outer membrane leaflet sphingolipid GM1 have a conical intrinsic shape (Hirai et al. 1998, 2003), it should not coalesce in the inward curved regions of membrane invaginations. We can only speculate that GM1-specific rafts coalesce in the more outward bent membrane necks of small invaginations. Alternatively, it can be speculated that, upon stomatocytogenic amphiphile treatment, GM1-containing rafts attract specific membrane components to the corresponding cytosolic face thereby altering the intrinsic curvature of these rafts ($C_{1m} < 0$ and/or $C_{2m} < 0$). Previous studies have shown that raft-associated components, e.g., the glycosphingolipid globoside, cholesterol, and different host proteins sort into human erythrocyte malarial vacuolar invaginations (Lauer et al. 2000). In malarial endovacuoles, enrichment of flotillin-1, an oligomeric integral host raft protein (Salzer & Prohaska 2001) of the host membrane, was reported (Murphy et al. 2004). In contrast, we could not detect a consistent enrichment of flotillin-1 in amphiphile-induced invaginations (Figure 2D1). Nagao et al. (2002) suggested that malarial endovacuoles can recruit flotillin-1 because *Plasmodium falciparum* infection disrupts the association of flotillin-1 with erythrocyte rafts by reducing the cholesterol and sphingomyelin levels of the host erythrocyte membrane. In line with studies on malarial endovacuoles (Murphy et al. 2004), no enrichment of stomatin was observed in amphiphile-induced invaginations (Figure 2E1). The preferential distribution of BODIPY-GM1 in invaginations (Figure 2C1 and 2C2) and not in exvaginations is in line with the idea of a curvature-dependent lateral distribution of membrane components. Namely, the fluorophore group of the BODIPY-GM1 complex should increase the volume of the hydrophobic part of GM1 and thereby change its molecular shape in the direction toward an inverted conical shape (with $C_{1m} < 0$ and/or $C_{2m} < 0$).

The non-homogeneous lateral distribution of membrane (raft) components has been recently indicated also in Golgi vesicles, where some of the membrane components may be concentrated mainly on the highly curved bulbous rims of the Golgi vesicles, while other components are distributed predominantly in their flat central part (Sprong et al. 2001, Iglič et al. 2004). The variation of the lateral composition of the membrane over the membrane surface may determine the location of the membrane bud, or the site of the fusion of the carrier vesicle with the organelle membrane (Sprong et al. 2001).

Understanding the mechanism that maintains the non-homogeneous lateral distribution of lipids and proteins in biological membranes provides a major challenge in current cell biology and the precise mechanism by which it is accomplished remains to be established (Hägerstrand et al. 2004, McMahon & Gallop 2005, Fošnarič et al. 2005, Zimmerberg & Kozlov 2006, Iglič et al. 2006). In this work, possible physical mechanisms maintaining the non-homogeneous lateral distribution of the membrane proteins and lipids are proposed. We present a hypothesis that successfully explains the coupling of the observed non-homogeneous lateral distribution of the rafts and the local membrane shape. In spite of the complexity of the real system and the simplifications assumed in our theoretical model of the membrane, the presented experimental and theoretical results may lead to a better understanding of the mechanisms that maintain the non-homogeneous lateral distribution of the rafts in biological membranes.

Acknowledgements

L.M. is grateful to CIMO and the Academy of Finland for financial support. A.I. was supported by the Åbo Akademi University. U.S. and R.P. were supported by the Austrian Science Fund (FWF). We are grateful to Gunilla Henriksson, Esa Nummelin, Tomas Bymark, Blaž Babnik and Miha Fošnarič for technical assistance and help with calculations. We are indebted to the Oskar Öflund Foundation, the Research Institute and the Rector at the Åbo Akademi University for their financial support.

References

Allan D, Billah MM, Finean JB, Michell RH. 1976. Release of diacylglycerol-enriched vesicles from erythrocytes with increased intracellular (Ca^{2+}). Nature 261:58–60.

Allan D, Thomas P. 1981. Ca^{2+}-induced biochemical changes in human erythrocytes and their relation to microvesiculation. Biochem J 198:433–440.

Allan D, Thomas P, Limbrick AR. 1980. The isolation and characterization of 60 nm vesicles ('nanovesicles') produced during ionophore A23187-induced budding of human erythrocytes. Biochem J 188:881–887.

Bohinc K, Kralj-Iglič V, May S. 2003. Interaction between two cylindrical inclusions in symmetric lipid bilayer. J Chem Phys 119:7435–7444.

Corbeil D, Röper K, Fargeas CA, Joester A, Huttner WB. 2001. Prominin: a story of cholesterol, plasma membrane protrusions and human pathology. Traffic 2:82–91.

Deuticke B. 1968. Transformation and restoration of biconcave shape of human erythrocytes induced by amphiphilic agents and changes of ionic environment. Biochim Biophys Acta 163:494–500.

Devaux PF, Morris R. 2004. Transmembrane asymmetry and lateral domains in biological membranes. Traffic 5:241–246.

Fošnarič M, Bohinc K, Gauger DR, Iglič A, Kralj-Iglič A, May S. 2005. The influence of anisotropic membrane inclusions on

curvature elastic properties of lipid membranes. J Chem Inf Model 45:1652–1661.

Hagelberg C, Allan D. 1990. Restricted diffusion of integral membrane proteins and polyphosphoinositides leads to their depletion in microvesicles released from human erythrocytes. Biochem J 271:831–834.

Harder T, Scheiffele P, Verkade P, Simons K. 1998. Lipid domain structure of the plasma membrane revealed by patching of membrane components. J Cell Biol 141:929–942.

Herr C, Clemen CS, Lehnert G, Kutschkow R, Picker SM, Gathof BS, Zamparelli C, Schleicher M, Noegel AA. 2003. Function, expression and localization of annexin A7 in platelets and red blood cells: insights derived from an annexin A7 mutant mouse. BMC Biochemistry 4(8). Available: http://www.biomedcentral.com/1471-209/4/8. Accessed 19 August 2003.

Hiebl-Dirschmied CM, Entler B, Glotzmann C, Maurer-Fogy I, Stratowa C, Prohaska R. 1991. Cloning and nucleotide sequence of cDNA encoding human erythrocyte band 7 integral membrane protein. Biochim Biophys Acta 1090:123–124.

Hill TL. 1986. An introduction to statistical thermodynamics. New York: Dover Publications.

Hirai M, Iwase H, Arai S, Takizawa T, Hayashi K. 1998. Interaction of ganglioside with proteins depending on oligosaccharide chain and protein surface modification. Biophys J 74:1380–1387.

Hirai M, Iwase H, Hayakawa T, Koizumi M, Takahashi H. 2003. Determination of asymmetric structure of ganglioside-DPPC mixed vesicle using SANS, SAXS and DLS. Biophys J 85:1600–1610.

Huttner WB, Zimmerberg J. 2001. Implications of lipid microdomains for membrane curvature, budding and fission. Curr Opin Cell Biol 13:478–484.

Hägerstrand H, Danieluk M, Bobrowska-Hägerstrand M, Iglič A, Wróbel A, Isomaa B, Nikinmaa M. 2000. Influence of band 3 protein absence and skeletal structures on amphiphile- and Ca^{2+}-induced shape alterations in erythrocytes – a study with lamprey (*Lampetra fluviatilis*), trout (*Oncorhynchus mykiss*) and human erythrocytes. Biochim Biophys Acta 1466:125–138.

Hägerstrand H, Isomaa B. 1989. Vesiculation induced by amphiphiles in erythrocytes. Biochim Biophys Acta 982:179–186.

Hägerstrand H, Isomaa B. 1992. Morphological characterization of exovesicles and endovesicles released from human erythrocytes following treatment with amphiphiles. Biochim Biophys Acta 1109:117–126.

Hägerstrand H, Isomaa B. 1994. Lipid and protein composition of exovesicles induced by amphiphiles in human erythrocytes. Biochim Biophys Acta 1190:405–415.

Hägerstrand H, Kralj-Iglič V, Fošnarič M, Bobrowska-Hägerstrand M, Wróbel A, Mrówczynska L, Söderström T, Iglič A. 2004. Endovesicle formation and membrane perturbation induced by polyoxyethyleneglycolalkylethers in human erythrocytes. Biochim Biophys Acta 1665:191–200.

Iglič A. 1997. A possible mechanism determining the stability of spiculated red blood cells. J Biomech 30:35–40.

Iglič A, Babnik B, Bohinc K, Fošnarič M, Hägerstrand H, Kralj-Iglič V. 2006. On the role of anisotropy of membrane constituents in formation of a membrane neck during budding of a multicomponent membrane. J Biomech (In press)

Iglič A, Hägerstrand H. 1999. Amphiphile-induced spherical microvesicle correspond to an extreme local area difference between two monolayers of the membrane bilayer. Med Biol Eng Comput 37:125–129.

Iglič A, Fošnarič M, Hägerstrand H, Kralj-Iglič V. 2004. Coupling between vesicle shape and the non-homogeneous lateral distribution of membrane constituents in Golgi bodies. FEBS Lett 574:9–12.

Ikonen E. 2001. Roles of lipid rafts in membrane transport. Curr Opin Cell Biol 13:470–477.

Janes PW, Ley SC, Magee AI. 1999. Aggregation of lipid rafts accompanies signaling via the T cell antigen receptor. J Cell Biol 147:447–461.

Kamp D, Sieberg T, Haest CW. 2001. Inhibition and stimulation of phospholipid scrambling activity. Consequences for lipid asymmetry, echinocytosis, and microvesiculation of erythrocytes. Biochemistry 40:9438–9446.

Kralj-Iglič V, Hägerstrand H, Veranič P, Jezernik K, Babnik B, Gauger DR, Iglič A. 2005. Amphiphile-induced tubular budding of the bilayer membrane. Eur Biophys J 34:1066–1070.

Lauer S, VanWye J, Harrison T, McManus H, Samuel BU, Hiller NL, Mohandas N, Haldar K. 2000. Vacuolar uptake of host components, and a role for cholesterol and sphingomyelin in malarial infection. EMBO J 19:3556–3564.

Liemann S, Bringemeier I, Benz J, Gottig P, Hofmann A, Huber R, Noegel AA, Jacob U. 1997. Crystal structure of the C-terminal tetrad repeat from synexin (annexin VII) of Dictyostelium discoideum. J Mol Biol 270:79–88.

Lim HWG, Wortis M, Mukhopadhyay R. 2002. Stomatocyte-discocyte-echinocyte sequence of the human red blood cell: evidence for the bilayer-couple hypothesis from membrane mechanics. Proc Natl Acad Sci USA 99:16766–16769.

Lin S, Yang E, Huestis WH. 1994. Relationship of phospholipid distribution to shape change in Ca^{2+}-crenated and recovered human erythrocytes. Biochemistry 33:7337–7344.

Liu SC, Derick LH, Duquette MA, Palek J. 1989. Separation of lipid bilayer from the membrane skeleton during discocyte-echinocyte transformation of human erythrocyte ghost. Eur J Cell Biol 49:358–365.

Mairhofer M, Steiner M, Mosgoeller W, Prohaska R, Salzer U. 2002. Stomatin is a major lipid-raft component of platelet alpha granules. Blood 100:897–904.

McMahon HT, Gallop JL. 2005. Membrane curvature and mechanisms of dynamic cell membrane remodelling. Nature 438:590–596.

Mukhopadhyay R, Lim HWG, Wortis M. 2002. Echinocyte shapes: bending, stretching, and shear determine spicule shape and bending. Biophys J 82:1756–1772.

Murphy SC, Samuel BU, Harrison T, Speicher KD, Speicher DW, Reid ME, Prohaska R, Low PS, Tanner MJ, Mohandas N, Haldar K. 2004. Erythrocyte detergent-resistant membrane proteins: their characterization and selective uptake during malarial infection. Blood 103:1920–1928.

Nagao E, Seydel KB, Dvorak JA. 2002. Detergent-resistant erythrocyte membrane rafts are modified by a *Plasmodium falciparum* infection. Exp Parasitol 102:57–59.

Neumann-Giesen C, Falkenbach B, Beicht P, Claasen S, Lüers G, Stuermer CA, Herzog V, Tikkanen R. 2004. Membrane and raft association of reggie-1/flotilin-2: role of myristoylation, palmitoylation and oligomerization and induction of filopodia by overexpression. Biochem J 378:509–518.

Plowman SJ, Muncke C, Parton RG, Hancock JF. 2005. H-ras, K-ras, and inner plasma membrane raft proteins operate in nanoclusters with differential dependence on the actin cytoskeleton. Proc Natl Acad Sci USA 102:15500–15505.

Pralle A, Keller P, Florin EL, Simons K, Horber JK. 2000. Sphingolipid-cholesterol rafts diffuse as small entities in the plasma membrane of mammalian cells. J Cell Biol 148:997–1008.

Prior IA, Muncke C, Parton RG, Hancock JF. 2003. Direct visualization of Ras proteins in spatially distinct cell surface microdomains. J Cell Biol 160:165–170.

Rety S, Sopkova-de Oliveira Santos J, Dreyfuss L, Blondeau K, Hofbauerova K, Raguenes-Nicol C, Kerboeuf D, Renouard M, Russo-Marie F, Lewit-Bentley A. 2005. The crystal structure of annexin A8 is similar to that of annexin A3. J Mol Biol 345:1131–1139.

Rajendran L, Masilamani M, Solomon S, Tikkanen R, Stuermer CA, Plattner H, Illges H. 2003. Asymmetric localization of flotillins/reggies in preaseembled platforms confers inherent polarity to hematopoietic cells. Proc Natl Acad Sci USA 100:8241–8246.

Röper K, Corbeil D, Huttner WB. 2000. Retention of prominin in microvilli reveals distinct cholesterol-based lipid microdomains in the apical plasma membrane. Nat Cell Biol 2:582–592.

Sprong H, van der Sluijs P, van Meer G. 2001. How proteins move lipids and lipid move proteins. Nat Cell Biol 2:504–513.

Salzer U, Prohaska R. 2001. Stomatin, flotillin-1, and flotillin-2 are major integral proteins of erythrocyte lipid rafts. Blood 97:1141–1143.

Salzer U, Prohaska R. 2003. Segregation of lipid raft proteins during calcium-induced vesiculation of erythrocytes. Blood 101:3751–3753.

Salzer U, Hinterdorfer P, Hunger U, Borken C, Prohaska R. 2002. Ca^{++}-dependent vesicle release from erythrocytes involves stomatin-specific lipid rafts, synexin (annexin VII), and sorcin. Blood 99:2569–2577.

Sharma P, Varma R, Sarasij RC, Ira, Gousset K, Krishnamoorthy G, Rao M, Mayor S. 2004. Nanoscale organization of multiple GPI-anchored proteins in living cell membranes. Cell 116:577–589.

Sheetz MP, Singer SJ. 1976. Equilibrium and kinetic effects of drugs on the shapes of human erythrocytes. J Cell Biol 70:247–251.

Simons K, Vaz WL. 2004. Model systems, lipid rafts, and cell membranes. Annu Rev Biophys Biomol Struct 33:269–295.

Simons K, Toomre D. 2000. Lipid rafts and signal transduction. Nat Rev Mol Cell Biol 1:31–39.

Smeets EF, Comfurius P, Bevers EM, Zwaal RF. 1994. Calcium-induced transbilayer scrambling of fluorescent phospholipid analogs in platelets and erythrocytes. Biochim Biophys Acta 1195:281–286.

Staneva G, Seigneuret M, Koumanov K, Trugnan G, Angelova MI. 2005. Detergents induce raft-like domains budding and fission from giant unilamellar heterogeneous vesicles: a direct microscopy observation. Chem Phys Lip 136:55–66.

Zimmerberg J, Kozlov MM. 2006. How proteins produce cellular membrane curvature. Nat Rev Mol Cell Biol 7:9–19.

Appendix

Theoretical considerations

In the Appendix, the curvature and direct interactions induced accumulation of raft elements is discussed theoretically. In the theoretical considerations, we use the term 'raft element' to specifically address a small raft entity with specific lipid and protein composition and specific intrinsic shape. Raft element is in general not rigid and can adjust its shape by bending. Larger raft domains result from the aggregation of many raft elements of the same and/or of different type(s).

It was previously indicated that clustering of small mobile raft elements into larger raft domains may be induced by a membrane bending and/or attractive forces between molecules (Harder et al. 1998 and references therein). Interestingly, it was shown that overexpression of flotillin results in the induction of numerous thin tubular membrane protrusions (Neumann-Giesen et al. 2004). In this process the lipid-flotillin complex formation and flotillin oligomerization seems to play an important role. Similarly, accumulation of specific prominin rafts on highly curved membrane protrusions has been recently indicated (Corbeil et al. 2001). Therefore it was suggested that prominin rafts play an important role in stabilization of plasma membrane protrusions (Huttner & Zimmerberg 2001). Since prominin is not directly interacting with the actin-based cytoskeleton (Huttner & Zimmerberg, 2001), the predominant localization of prominin in protrusions may be explained by the curvature-induced accumulation of prominin rafts with the intrinsic shape of prominin rafts representing the main driving force. The redistribution of prominin after mild cholesterol depletion from the protrusions indicates the importance of cholesterol (Röper et al. 2000) and other lipids as partners (Huttner & Zimmerberg, 2001) in the formation of small rafts. Moreover, the non-homogeneous lateral distribution of flotillins and their accumulation during cytokinesis was observed recently (Rajendran et al. 2003).

To better understand the physical mechanism that may induce the observed clustering of raft markers in erythrocyte membrane and in spherical membrane vesicles, we consider a simple theoretical model, where the normalised free energy of membrane isotropic raft elements f_{in} is written in the form:

$$f_{in} = kT\int n \ln n \, da + kT \int (1-n)\ln(1-n)\, da + 2w\int n^2 \, da + \int \frac{\xi}{2} n(H-H_m)^2 \, da. \quad (1)$$

Here, $n(\mathbf{r})$ is the fraction of the membrane area covered by raft elements at the given position $\mathbf{r}$, ξ is the constant describing the strength of the interaction between the raft elements and the curvature field of the membrane (Iglič et al. 2004), kT is the thermal energy, w is the interaction energy between two neighbouring raft elements (see also Hill, 1986), $H=(C_1+C_2)/2$ is the mean curvature and $H_m = (C_{1m}+C_{2m})/2$ is the mean curvature describing the intrinsic shape of the raft elements (Figure 4) (Iglič et al. 2004). Intrinsic curvatures C_{1m} and C_{2m} are the principal curvatures of the raft element (Figure 4) which corresponds to the minimal possible energy of the raft element including its bending energy and the energy of the surrounding disturbed membrane

molecules (lipids). Integration goes over the entire (normalized) area of the membrane surface ($a = 1$). The first two terms in Equation (1) represent the configurational entropy of raft elements.

By taking into account the conservation equation for all raft elements $\int n \, \mathrm{d}a = \overline{n}$, where $\overline{n}$ is the average value of n, a functional is constructed: $\int (f_{in} + \lambda n)\mathrm{d}a = \int L(n) \, \mathrm{d}a$, where λ is the Lagrange parameter. Variation is performed by solving the corresponding Euler equation $\partial L/\partial n = 0$ which gives:

$$n = \frac{\vartheta \exp(-\beta)}{1 + \vartheta \exp(-\beta)} \times \left[1 - \frac{4w}{kT} \frac{\vartheta \exp(-\beta)}{(1 + \vartheta \exp(-\beta))^2}\right], \quad (2)$$

where $\beta = \xi(H(\mathbf{r}) - H_m)^2/2kT$ and $\vartheta = \exp(-\lambda)$. In the above expression the nonlinear terms in w are neglected. The parameter ϑ is determined from the condition $\int n \, da = \overline{n}$.

Equation (2) shows that the fraction of the membrane area covered by the raft elements (n) may locally increase dramatically if the local membrane curvature $H(\mathbf{r})$ approaches the intrinsic curvature of the raft nanodomains H_{m}. For high enough values of H and H_{m} the value of n approaches unity indicating the possibility of a complete lateral phase separation and formation of large raft domains. The effect may be further accelerated by attractive nearest-neighbour interactions ($w < 0$) between the neighbouring raft elements. The predicted curvature (and direct interactions) induced coalescence of raft elements (Equation (2)) corresponds well to the observed clustering of raft elements in caveolae (Figure 5) which may function as traps for raft elements (Harder et al. 1998). It can be seen in Equation (2) that clustering of raft elements may take place also without membrane bending, solely due to attractive forces ($w < 0$) between the neighbouring raft elements. The presented theoretical model (Equation (2)) may thus offer the possible theoretical explanation for the enrichment of raft elements in highly curved membrane regions (Table II) and for the coalescence of raft elements in nearly flat membrane regions (Figure 1B2, 2D1 and 2E1) due to attractive forces. Abolishing the membrane skeleton-raft component interactions (as for example due to partial membrane skeleton detachment (Liu et al. 1989)) should increase the lateral mobility of raft elements and thereby their ability to sort due to membrane curvature and/or direct interactions. Notably, attractive forces between two raft components can be mediated by other membrane constituents (Bohinc et al. 2003).

The local mechanical properties and curvature of the membrane may be strongly influenced by the size and lateral distribution of the membrane elements (Iglič et al. 2004). Based on Equations (1) and (2) it can be concluded that formation of membrane vesicles may be affected or driven by the lateral redistribution (or segregation) of the raft elements (Figure 5), where the size of the spherical vesicles is directly related to the intrinsic (spontaneous) curvature of the membrane (raft) elements $H_{\mathrm{m}} = (C_{1\mathrm{m}} + C_{2\mathrm{m}})/2$.

In addition, due to accumulation of isotropic conical membrane elements in the budding region (Figure 5), the budding process may be driven also by accumulation of anisotropic membrane components in the neck connecting the bud and the parent membrane (Iglič et al. 2006) and by a local change of the area difference between the outer and inner lipid layer (Iglič & Hägerstrand 1999, Staneva et al. 2005).